Original Research Article

Expression of 1L-myo-Inositol -1-Phosphate Synthase (EC 5.5.1.4) is Deregulated in the Cerebellum of Curly Tail Mutant Mice

ABSTRACT

Previous research, defining spatial control of inositol phosphate biosynthesis in the developing brain of CBA (normal) and CT [curly tail (ct-CT) and straight tail (st-CT)] mutant mice implicated a role for 1l-myo-inositol 1-phosphate synthase (MIP) in normal functioning of the central nervous system. Biochemical research indicated that MIP enzymatic activity, conversion of glucose 6-phosphate into inositol phosphate, is highest in the cerebellum of ct-CT and lowest in st-CT, when compared to that of CBA mice.

Here, we utilized microscopic and biochemical investigations to analyze and extend previous findings of MIP expression in the cerebellum. Results of this research indicated that MIP expression correlates, well, with its enzymatic activity in the cerebellum of CBA and CT mutant mice. Statistical analyses of fluorescent micrographs detected a significant difference in fluorescence intensity between MIP from ct-CT, st-CT, and CBA mice.

These data support vital links between inositol phosphate biosynthesis, MIP expression, and normal functioning of the cerebellum. Moreover, published data, identifying significant behavioral differences in the CT mutant, as well as data linking motor and non-motor cerebellar functions to abnormal levels of inositol, support the conclusion that aspects of normal cerebellar functions require temporal and spatial control of inositol phosphate biosynthesis, MIP expression.

Keywords

Cerebellum, CBA, ct-CT mutant, st-CT mutant, 1L-myo-Inositol -1-Phosphate Synthase

1. Introduction

Recent advances in neurological disorder research support a critical role for inositol in the mammalian central nervous system (CNS). Elevated inositol levels have been correlated with a number of neurological disorders, including panic disorder, obsessive-compulsive disorder, and multiple sclerosis (Colodny and Hoffman, 1998; Vawter et al., 2019). For example, it has been shown that myo-inositol concentration levels are increased in the frontal cortex in children with a mood disorder compared with healthy children (Cecil et al., 2003). In addition, elevated concentrations of myo-inositol were detected in the anterior cingulate of bipolar adolescents when compared to healthy individuals (Strakowski et al., 2005). Remarkably, highly increased levels of myo-inositol were found in cerebral white matter in a new Vsyndrome characterized by hypomyelination with atrophy of the basal ganglia and the cerebellum (van der Knaap et al., 2002), while others have recently shown that a phosphorylator of inositol, inositol hexakisphosphate kinase-2 in cerebellar granule cells, regulates Purkinje cell morphology and cerebellar synapses (Nagpal et al., 2018). Determining myo-inositol concentration during human brain development provides essential clues concerning its functions in the cerebellum (Kreis et al., 1993; Dineen et al., 2019) and allows subsequent, non-invasive therapeutic intervention.

The biosynthesis of inositol phosphate is catalyzed by myo-inositol 1-phosphate synthase (MIP) (Loewus and Loewus, 1983; Eisenberg, 1967). The overall reaction mechanism consists of a tightly coupled oxidation and reduction (Loewus and Loewus, 1983; Eisenberg, 1967; Sherman et al., 1969). A major nutritionally active form of inositol, myo-inositol, is vital to many

neurological processes (Holub, 1982; Cavalli and Copp, 2002; Groenen et al., 2004; Greene et al., 2017).

In 1998, Briner and Peterson (Briner and Peterson, 1998) compared the behavior of CT mutant mice, which are susceptible to inositol supplementation, but resistant to folic acid treatment for spina bifida (Greene and Copp, 1997), with that of normal CBA mice. They observed significant behavioral differences, with the CT strain being hyperactive, hyperreactive, and memory deficient. These results correlate well with our finding that there is a significantly higher level of inositol, overall, in the ct-CT cerebellum when compared to levels of inositol in the cerebellum of CBA and st-CT mice (Alebous, 2009). Given the number of published reports documenting the crucial roles of inositol in the CNS and findings that suggest inositol supplementation reduces neural tube defects (NTDs) (Greene and Copp, 1997), it was vital to ask questions concerning the spatial control of de novo inositol phosphate biosynthesis in the developing mammalian brain (Alebous, 2009). Microscopic studies presented here extend biochemical results, which revealed that there is a significantly lower level of inositol, overall, in the st-CT cerebellum when compared to levels of inositol in the cerebellum of CBA and ct-CT mice (Alebous, 2009). No significiant difference in levels of inositol was detected in the cerebrum of CBA, st-CT, and st-CT.

2. Experimental procedure

2.1 Mouse Brains

Adult ct-CT (STOCK-ct/ct-JAX catalog), adult st-CT (STOCK-ct/ct-JAX catalog) and CBA mice (CBA/CaGnle strain) were generously donated by Dr. Muriel T. Davisson, Director of the Genetics Center at the Jackson Laboratory (Bar Harbor, Maine USA). Mice were decapitated in

accordance with the “Guide for the Care and Use of Laboratory Animals at the Jackson Laboratory” (Bar Harbor, MA, USA). All adult mouse cerebellar regions were removed, frozen in liquid nitrogen, and stored at -80°C prior to use.

2.2. Morphology of Cerebellum

To examine differences in morphology of the adult mouse cerebellum, sections were stained with haematoxylin and eosin (H&E), viewed with an Axioskop Zeiss microscope, and photographed with an Axiocam HRc Zeiss camera.

2.3. Immunohistochemistry

The cerebellum of adult CBA, st-CT, and ct-CT mice was fixed in 3.7% formaldehyde (v/v) and 5% acetic acid (v/v) in 0.1 M sodium phosphate buffer (pH 7.2) for 48 h at 4°C. The fixative was removed, and tissue dehydrated in a graded series of ethanol (50% for 30 min, 2 x 70% for 1 h, 90% for 2 h, 2 x 100% for 2 h) and chloroform (16 h). Tissues were incubated overnight in paraffin at 62°C and embedded in paraffin blocks. Sections (5 µm) were cut transversely from chilled trimmed blocks on a Leica Micro R.M 2135 microtome, at UAB, floated onto poly-D-Lysine coated slides (50 µg/mL poly-D-lysine in 10 mM Tris–HCl, pH 8.0) and air-dried for 2 h. Sections were rehydrated for 3 min in 100%, 95%, 75%, 50%, and 25% ethanol, dH2O, and TBS, after paraffin removal by 2 x 3 min rinses in Safe Clear Tissue Clearing Agent (Fisher). Subsequently, sections were blocked for 30 min in TTBS (TBS with 0.01% Tween 20) and incubated overnight in a humidity chamber with rabbit polyclonal anti-yeast MIP antibody (1:500 dilution). Unbound primary antibody was removed with 3 x 15 min rinses in TTBS, with gentle agitation. Finally, sections were reblocked 30 min in TTBS, and sheep anti-rabbit IgG (whole molecule) Cy3-conjugated (1:1000 dilution) was added for 2 h in a humidity chamber at room temperature, rinsed 3 x 15 min in TTBS with gentle agitation, 1 min in dH2O, and allowed

to dry briefly. To control for nonspecific binding of the Cy3-conjugated secondary antibody, MIP primary antibody was omitted from control sections. For each mouse, six different fields were viewed with an Axioskop Zeiss microscope and photographed using an Axiocam HRc Zeiss camera.

2.4. Immunohistochemistry

Expression of MIP was analyzed using ImageJ software (version 1.48v; Rasband, W.S., ImageJ, U. S. National Institutes of Health, Bethesda, Maryland, USA, http://imagej.nih.gov/ij/, 1997-2014). Resulting data were fed into a Statistical Package for the Social Science (SPSS 20) software and analyzed using descriptive analysis and One-Way Analysis of Variance (ANOVA). A p value <0.05 was considered statistically significant.

2.5. Protein Isolation

Proteins from the cerebellum of CBA, ct-CT, and st-CT adult mice were isolated according to the method of Ping et al. (1999). Tissue, 0.03 g per sample, was ground to a powder with a pestle and mortar containing liquid nitrogen and resuspended in 1 ml of 1x homogenization buffer Tris buffered saline (TBS), 10 mM Tris-HCl,150 mM NaCl pH 7.5], 1% Triton–X100, and one tablet of protease inhibitor [complete mini, EDTA-free, protease inhibitor cocktail (Roche)] per 10 ml of buffer. Samples were vortexed for 5 min, centrifuged at a maximum of 14,000 rpm (Eppendorf centrifuge) for 5 min, and supernatant removed and transferred to a clean tube. After addition of another 1 ml of homogenization buffer, the pellet was resuspended, centrifuged as above, and supernatant added to previously isolated 1 ml. Proteins were precipitated overnight from 2 ml of supernatant at -20°C, using 8 ml of ice-cold acetone containing 10 mM ß-mercaptoethanol. To pellet proteins, samples were centrifuged for 5 min at 5,000 rpm (IEC clinical centrifuge), and the supernatant was removed. After reconstituting the pellet in 100 µl of

homogenization buffer, protein concentrations were measured using Bio-Rad protein assay based on the method of Bradford 1976.

2.6. Western Blotting

Proteins isolated from the cerebellum of CBA, ct-CT, and st-CT adult mice were utilized for Western blotting analyses; experiments were repeated a minimum of three times. Proteins (50 ug) were boiled (5 min) and loaded in sample buffer (25 mM Tris-HCl, 0.2 M glycine, and 0.1% SDS, pH 8.3). After that, samples were electrophoresed at 175 V for 6 h in an SDS-polyacrylamide gel according to the method of Laemmli (1970); the gel consisted of a 6% stacking gel and a 12.5% separating gel. Western blotting analyses were performed according to the method of Towbin (1979). Separated proteins were transferred overnight at 22 V in Tris–glycine buffer (25 mM Tris-HCl, 192 mM glycine, 20% methanol) onto a nitrocellulose membrane. The membrane was blocked at least 2 h in rinse buffer (0.1% Triton–X100, 10 mM Tris, 1 mM EDTA, 0.15 M NaCl) containing 5% (w/v) nonfat dry milk and incubated with yeast polyclonal MIP antibody (1:25,000 dilution) overnight at room temperature with constant agitation. Unbound antibody was removed by washing 3 x 15 min in rinse buffer. Subsequently, the membrane was reblocked 30 min, as previously described, incubated in goat anti-rabbit IgG conjugated peroxidase (1:6,000 dilution) for 2 h, and washed 3 x 30 min in rinse buffer. Bands were visualized by adding 2 ml of chemiluminescense reagents (Pierce) and exposing the membrane to X-ray film. After exposure, the membrane was washed with rinse buffer (5 min), stained (25% isopropanol, 10% glacial acetic acid, 0.01% amido black) for 1 min, and destained (25% isopropanol, 10% glacial acetic acid) to visualize proteins.

3. Results

4. Histomorphology of the Cerebellum

Histological sections of the adult CBA, ct-CT, and st-CT cerebellum were examined to determine morphological differences in this region using the light microscope. These evaluations detected no differences in the gross morphology between normal, CBA, and mutants, ct-CT and st-CT (Fig. 1). The cerebellum of all was divided into its distinct layers [white matter, molecular layer, and granule cell layer (packed with small, purple nerve cells)]. The normal pattern of follia, leaflike bundles of neurons, in the cerebellum showed no abnormalities.

3.2 Immunohistochemistry

MIP expression in the cerebellum of CBA, st-CT, and ct-CT adult mice was evaluated using immunohistochemistry. Differential expression of MIP (Fig. 2) was detected in the cerebellum of normal CBA and mutant curly tail adult mice.

Microscopic evaluations indicated that MIP expression in the cerebellum of ct-CT mice (Fig. 2, panels G- H) was higher than MIP expression in the cerebellum of CBA (Fig. 2, panels C- D) and st-CT mice (Fig. 2, panels E- F). One-Way ANOVA analyses were utilized to determine if observed fluorescence intensity differed significantly between normal and mutant mice. Statistically significant differences were detected between ct-CT and CBA as well as ct-CT and st-CT, $F(2, 24) = 7.444$, $p = 0.003$ (Fig. 3).

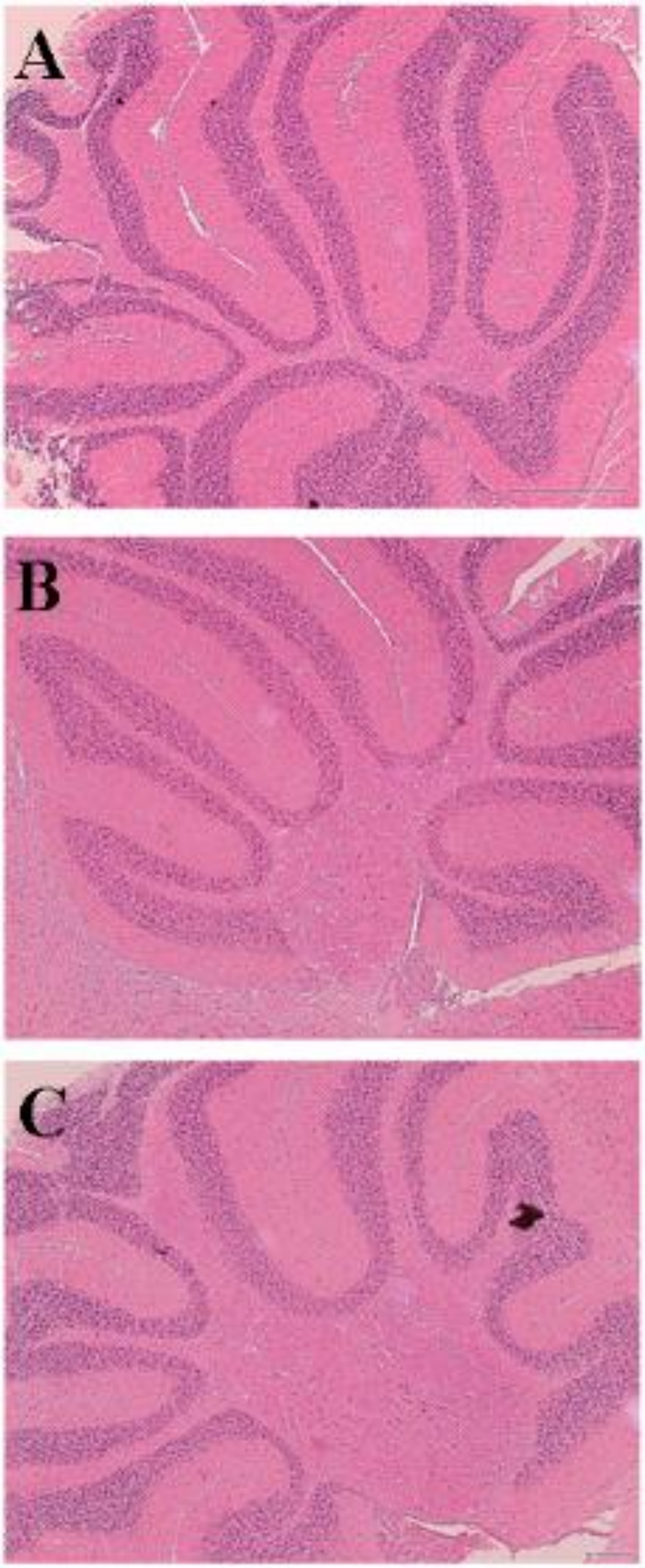
A
B
C

Fig. 1- Light Micrographs of the Mouse Cerebellum. Panels A, B, and C are 5 µm transverse sections of the cerebellum from CBA, st-CT, and ct-CT, respectively. Sections were stained with haematoxylin and eosin and visualized at 50X magnification. Bar = 500 µm for panel A. Bar = 200 µm for panels B and C.

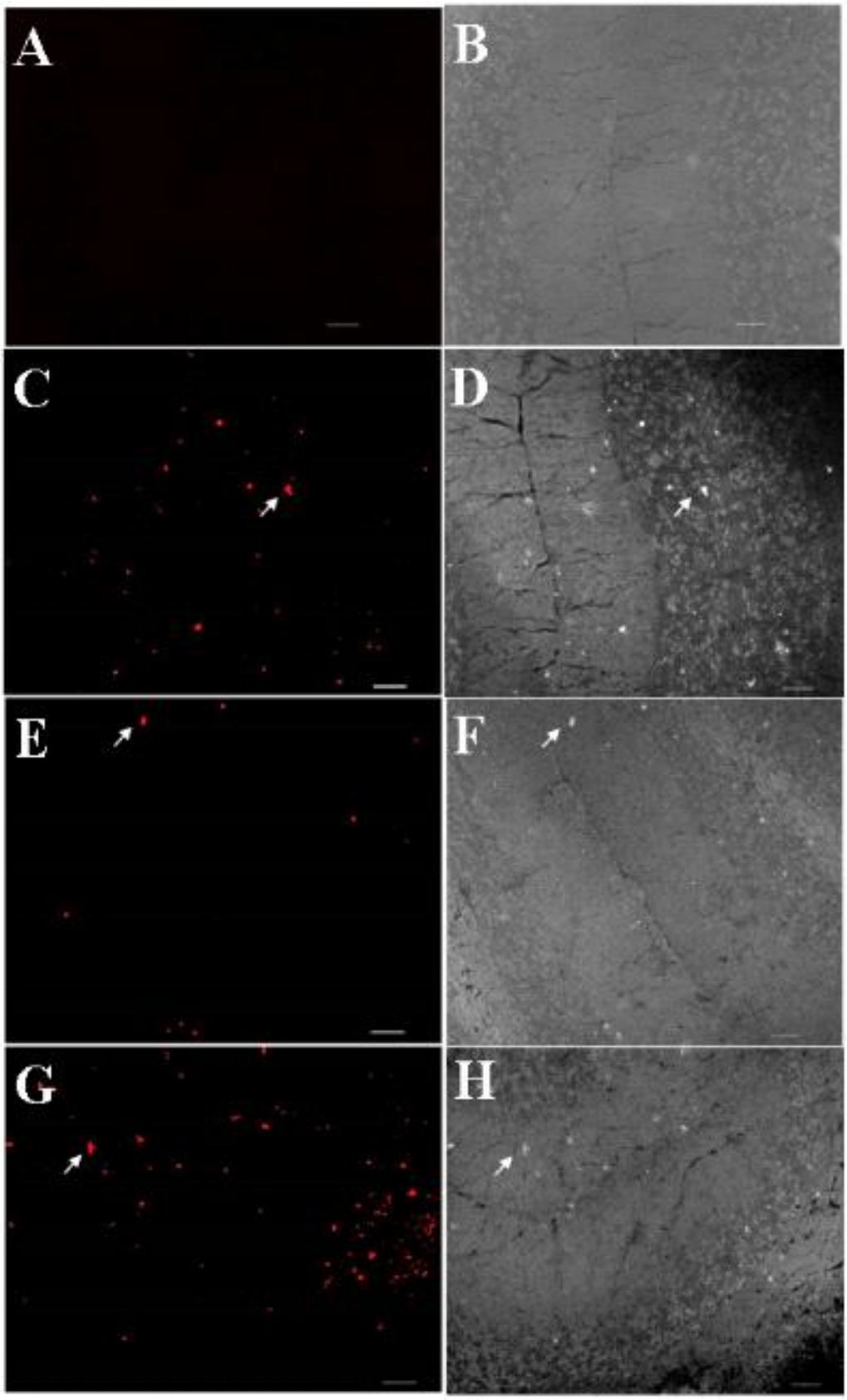
A
B
C
D
E
F
G
H

Fig. 2- Immunohistochemical Localization of MIP in the Adult Cerebellum. Panels A-H depict representative dual-channel fluorescent micrographs. MIP location in the same field of the cerebellum is indicated with (panels A, C, E, and G) and without (panels B, D, F, and H), the red channel. Expression of MIP is indicated by fluorescent particles as denoted with arrowheads. Sections were visualized at 20X magnification; Bar = 50 µm. Panels A and B illustrate typical control micrographs for nonspecific binding of the Cy3-conjugated secondary antibody; MIP antibody was omitted from control sections. Panels C and D display micrographs that exemplify patterns of MIP expression in the CBA cerebellum whereas panels E and F reflect a common expression pattern for MIP in the cerebellum of st-CT mice. A characteristic expression pattern of MIP in the ct-CT mouse cerebellum is shown in panels G and H.

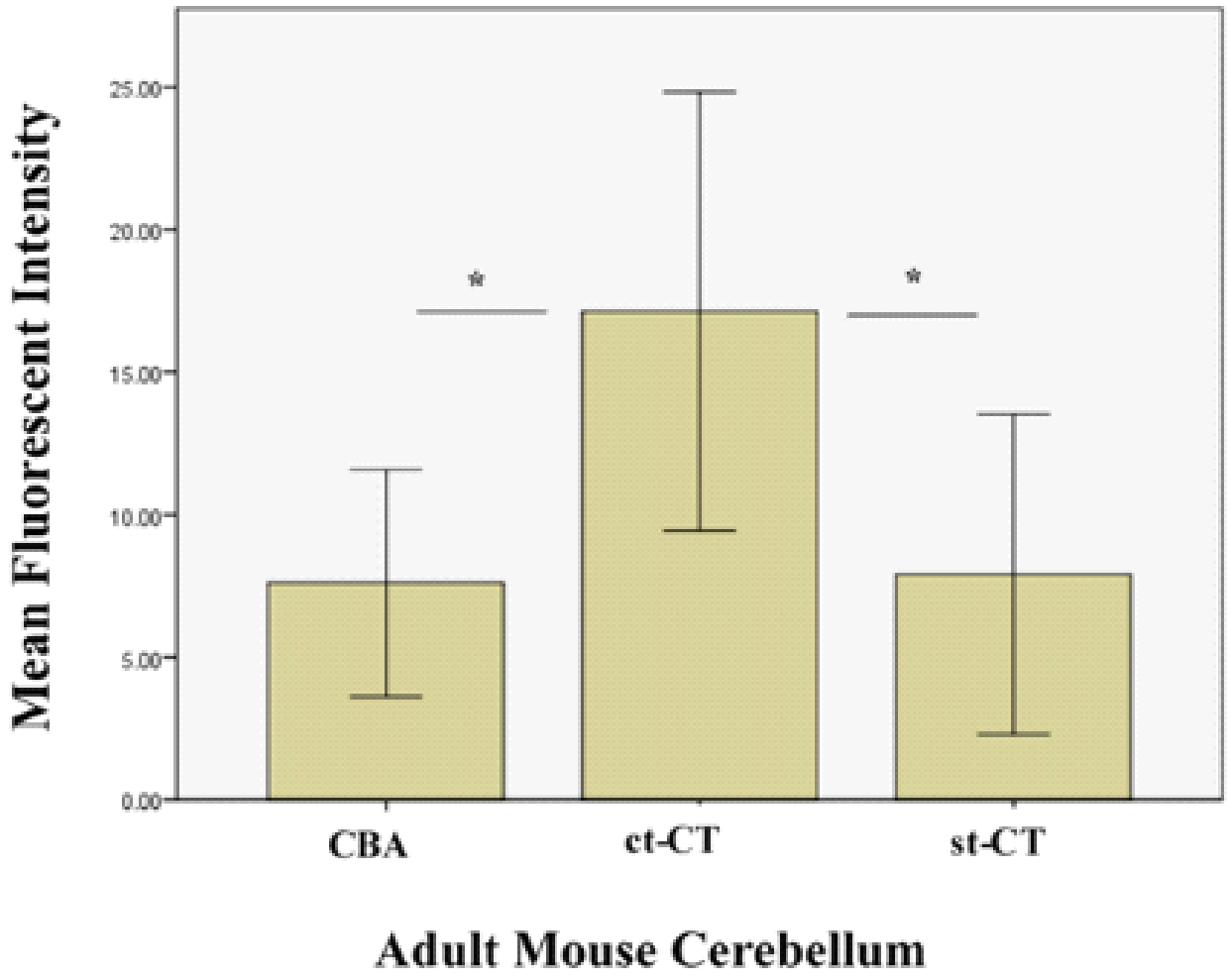

Fig. 3- Means of Fluorescence Intensity in the Cerebellum of Normal and Mutant Mice. Expression of MIP was analyzed in CBA, ct-CT and st-CT cerebellum using ImageJ software. * P value <0.05 was considered statistically significant. Error Bars: +/- 1 SD

3.3 Western Blotting

Western blotting analyses of proteins isolated from the cerebellum of CBA, st-CT, and ct-CT mice detected two differentially expressed isoforms of MIP, 33 kD and 20 kD proteins. Neither form was ever detectable in the cerebellum of st-CT adult mice (Fig. 4).

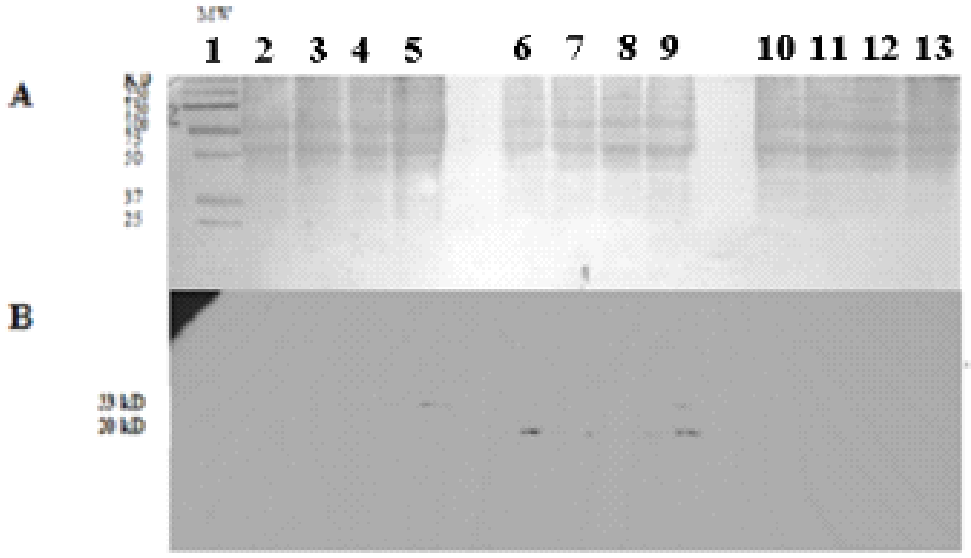

Fig. 4- MIP Antibody-Reactive Proteins in the Mouse Cerebellum. Panel A depicts a nitrocellulose membrane stained with Amido black dye. Lane 1 has molecular mass markers (MW); lanes 2-5, lanes 6-9, and lanes 10-13 contain cerebellum proteins isolated from adult CBA, ct-CT, and st-CT mice, respectively; all lanes contain 50 µg of protein. The chromatogram in Panel B shows MIP antibody-reactive cerebellum proteins of CBA (lane 5) and ct-CT (lanes 6-9) mice. Expression of the 33 kD or 20 kD MIP isoform was undetectable in the st-CT cerebellum (lanes 10-13).

5. Discussion

Studies of the cerebellum have extended its function of motor control to non-motor activities as well, including language, thought modulations, emotions and the ability to organize symbolic activities consecutively (Riva and Giorgi, 2000; Mitoma et al., 2020; Revuelta et al., 2020). Moreover, inositol metabolism has been connected to both motor and non-motor functions of the

cerebellum. For example, metabolomics analyses, using a mouse model of adult onset hypothyroidism (AOH), identified significant changes in cerebellar metabolic physiology that defined a physiological role for scyllo-inositol, an inositol isomer (Constantinou, 2010; Maga-Nteve et al. 2017). Research revealed that scyllo-inositol is the one metabolite that can differentiate between the euthyroid and the hypothyroid cerebellum (Constantinou, 2010). This observation provided a direct connection between AOH and cerebellar physiology. Importantly, myo-inositol is normally present in much higher concentrations in the cerebellum than scyllo-inositol and can be converted into scyllo- inositol through the action of a specific epimerase (Constantinou, 2010).

Findings from present research suggest that there are significant differences in inositol phosphate biosynthesis (MIP expression) in the cerebellum of ct-CT and st-CT mutant mice as compared to that of the healthy CBA mouse cerebellum. These results support a definitive connection between the regulation of inositol phosphate biosynthesis (MIP expression) and normal functioning of the cerebellum. Furthermore, other investigators have also demonstrated a link between aberrant inositol levels and cerebellar dysfunctions. For instance, research concerning sleep-onset rapid eye movement periods discovered increased cerebellar myo-inositol levels in two asymptomatic daughters with heterozygous DNMT1 mutations and a father with autosomal dominant cerebellar ataxia (Moghadam et al., 2014). Levels of myo- inositol in the cerebellum of the daughters were increased 38 and 52% when compared to gender and age-matched healthy controls (Moghadam et al., 2014). These findings provided additional support for utilizing aberrant levels of myo-inositol as a biomarker for abnormal cerebellar functions.

As with increased levels of myo-inositol, decreased levels of myo-inositol have also been attributed to cerebellar disorders. In fact, recent searches for biomarkers that can be utilized to

detect early symptoms for depression in schizophrenia indicated the potential use of myo-inositol (Chiappelli, 2015; Bustillo et al., 2019). Proton magnetic resonance spectroscopy was used to examine myo-inositol levels in the anterior cingulate cortex in 59 schizophrenia spectrum disorder patients and 69 matched community comparison participants (Chiappelli, 2015). Given the limitations of current tools being utilized to assess normal levels of myo-inositol in neurological disorders, it is reasonable to suggest that patients will benefit from assessing de novo inositol phosphate biosynthesis (MIP expression) as well. Results of present study advocate utilizing techniques that will allow investigators to generate a more holistic approach to studying normal and abnormal inositol metabolism in the mammalian brain. Specifically, future studies should not only quantitate levels of inositol but also query the regulation of its biosynthesis.

6. Conclusion

Results of present study concerning the spatial control of inositol biosynthesis in the cerebellum, further support the conclusion that altered levels of inositol during the formation and development of the mammalian brain produce numerous neurological disorders. Understanding mechanisms that regulate inositol biosynthesis in the developing brain will allow investigators to better assess and determine impact of inositol therapeutic intervention during human brain development.

COMPEING INTERESTS DISCLAIMER:

Authors have declared that no competing interests exist. The products used for this research are commonly and predominantly use products in our area of research and country. There is absolutely no conflict of interest between the authors and producers of the products because we do not intend to use these products as an avenue for any litigation but for the advancement of

knowledge. Also, the research was not funded by the producing company rather it was funded by personal efforts of the authors.

REFERENCES

Alebous, H.D., Cartee, R., Vaccari, D., Wright, O.A., Ahmed, A., Hood, R.D., Johnson, M.D., 2009. Developmental control of inositol phosphate biosynthesis is altered in the brain of both curly and phenotypically normal straight tail mutant mice. Birth Defects Research Part A: Clinical and Molecular Teratology. 85, 822-827.

Bradford, M.M., 1976. A rapid and sensitive method for the quantitation of microgram quantities of protein utilizing the principle of protein-dye binding. Analytical Biochemistry. 72, 248-254.

Briner, W., Peterson, S., 1998. Comparison of the behavior of the curly tail and CBA mouse on a neurologic scale. Neurotoxicol Teratol. 20,503–510.

Bustillo, JR., Jones, T., Qualls, C., Chavez, L., Lin, D., Lenroot, RK., Gasparovic, C., 2019. Proton magnetic resonance spectroscopic imaging of gray and white matter in bipolar-I and schizophrenia. Journal of affective disorders. 246:745-753.

Cavalli, P., Copp, A., 2002. Inositol and folate resistant neural tube defects. J Med Genet. 39,E5.

Cecil, K.M., DelBello, M.P., Sellars, M.C., Strakowski, S.M., 2003. Proton magnetic resonance spectroscopy of the frontal lobe and cerebellar vermis in children with a mood disorder and a familial risk for bipolar disorders. Journal of child and adolescent psychopharmacology. 13, 545-555.

Chiappelli, J., Rowland, L.M., Wijtenburg, S.A., Muellerklein, F., Tagamets, M.,

McMahon, R.P., Gaston, F., Kochunov, P., Hong, L.E., 2015. Evaluation of Myo-Inositol as a Potential Biomarker for Depression in Schizophrenia Neuropsychopharmacology. 40(9), 2157–2164.

Colodny, L., Hoffman, R.L., 1998. Inositol clinical applications for exogenous use. Altern Med Rev. 3,432–447.

Constantinou, C., Chrysanthopoulos, P.K., Margarity, M., Klapa, M.I., 2010. GC− MS metabolomic analysis reveals significant alterations in cerebellar metabolic physiology in a mouse model of adult onset hypothyroidism. Journal of proteome research. 10, 869-879.

Dineen, R. A., Raschke, F., McGlashan, H. L., Pszczolkowski, S., Hack, L., Cooper, A. D., Prasad, M., Chow, G., Whitehouse, W. P., Auer, D. P., 2019. Multiparametric cerebellar imaging and clinical phenotype in childhood ataxia telangiectasia. NeuroImage. Clinical, 25, 102110. Advance online publication.

Eisenberg, F. Jr., 1967. D-Myoinositol 1-phosphate as product of cyclization of glucose 6 phosphate and substrate for a specific phosphatase in rat testis. J Biol Chem. 242,1375–1382.

Greene, N.D., Copp, A.J. 1997. Inositol prevents folate-resistant neural tube defects in the mouse. Nat Med. 3,60–66.

Greene, N. D., Leung, K. Y., Copp, A. J., 2017. Inositol, neural tube closure and the prevention of neural tube defects. Birth defects research. 109(2), 68–80.

Groenen, P.M., Klootwijk, R., Schijvenaars, M.M., Straatman, H., Mariman, E.C., Franke, B., Steegers-Theunissen, R.P., 2004. Spina bifida and genetic factors related to myo-inositol, glucose, and zinc. Mol Genet Metab. 82,154–161.

Holub, B.J., 1982. The nutritional significance, metabolism, and function of myo-inositol and phosphatidylinositol in health and disease. Adv Nutr Res. 4,107–141.

Kreis, R., Ernst, T., Ross, B.D., 1993. Development of the human brain: in vivo quantification of metabolite and water content with proton magnetic resonance spectroscopy. Magnetic Resonance in Medicine. 30, 424-437.

Laemmli, U.K., 1970. Cleavage of structural proteins during the assembly of the head of bacteriophage T4. Nature. 227, 680-685.

Loewus, F., Loewus, M., 1983. Myo-inositol: It's biosynthesis and metabolism. Annu Rev Plant Physiol. 34,137–161.

Maga-Nteve, C., Vasilopoulou, CG ., Constantinou, C., Margarity, M., Klapa MI., 2016. Sex-comparative study of mouse cerebellum physiology under adult-onset hypothyroidism: The significance of GC-MS metabolomic data normalization in meta-analysis. Journal of chromatography. B, Analytical technologies in the biomedical and life sciences.1041-1042,158-166.

Mitoma, H., Manto, M., Gandini, J., 2020. Recent Advances in the Treatment of Cerebellar Disorders. Brain Sciences. 10(1). pii: E11.

Moghadam, K.K., Pizza, F., Tonon, C., Lodi, R., Carelli, V., Poli, F., Franceschini, C., Barboni, P., Seri, M., Ferrari, S., La Morgia, C., Testa, C., Cornelio, F., Liguori, R., Winkelmann, J., Lin, L., Mignot, E., Plazzi, G., 2014. Polysomnographic and neurometabolic features may mark preclinical autosomal dominant cerebellar ataxia, deafness, and narcolepsy due to a mutation in the DNA (cytosine-5-)-methyltransferase gene, DNMT1. Sleep medicine. 15, 582-585.

Nagpal, L., Fu, C., Snyder, S. H., 2018. Inositol Hexakisphosphate Kinase-2 in Cerebellar

Granule Cells Regulates Purkinje Cells and Motor Coordination via Protein 4.1N. The Journal of neuroscience : the official journal of the Society for Neuroscience. *38*(34), 7409–7419.

Ping, P., Zhang, J., Zheng, Y.T., Li, R.C., Dawn, B., Tang, X.L., Takano, H., Balafanova, Z., Bolli ,R., 1999. Demonstration of selective protein kinase C- dependent activation of Src and Lck tyrosine kinases during ischemic preconditioning in conscious rabbits. Circulation research. 85, 542-450.

Revuelta, M., Scheuer, T., Chew, L. Schmitz, T., 2020. Glial Factors Regulating White Matter Development and Pathologies of the Cerebellum. Neurochem Research . https://doi.org/10.1007/s11064-020-02961-z

Riva, D., Giorgi, C., 2000. The cerebellum contributes to higher functions during development Evidence from a series of children surgically treated for posterior fossa tumours. Brain. 123,1051-1061.

Sherman, W.R., Stewart, M.A., Zinbo, M., 1969. Mass spectrometric study on the mechanism of D-glucose 6-phosphate-L-myo-inositol 1-phosphate cyclase. J Biol Chem. 244,5703–5708.

Strakowski, S.M., Delbello, M.P., Adler, C.M., 2005. The functional neuroanatomy of bipolar disorder: a review of neuroimaging findings. Molecular psychiatry. 10,105-116.

Towbin, H., Staehelin, T., Gordon, J., 1979. Electrophoretic transfer of proteins from polyacrylamide gels to nitrocellulose sheets: Procedure and some applications. Proceedings of the National Academy of Sciences. 76, 4350-4354.

van der Knaap ,M.S., Naidu, S., Pouwels, P.J., Bonavita, S., van Coster, R., Lagae ,L., Sperner,

J., Surtees, R., Schiffmann, R., Valk, J., 2002. New syndrome characterized by hypomyelination with atrophy of the basal ganglia and cerebellum. American journal of neuroradiology. 23, 1466-1474.

Vawter, M.P., Hamzeh, A.R., Muradyan, E., Civelli, O., Abbott, G.W.' Alachkar, A., 2019. Association of Myoinositol Transporters with Schizophrenia and Bipolar Disorder: Evidence from Human and Animal Studies. Molecular Neuropsychiatry. 5,200 – 211.